*J. Chem. Sci.* Vol. 126, No. 1, January 2014, pp. 255–264. 

# Electron paramagnetic resonance study of ternary $Cu^{II}$ compounds with glycine and phenanthroline

RICARDO C SANTANA [a,*], ANDERSON B C ARAÚJO [a], JESIEL F CARVALHO [a] and RAFAEL CALVO [b]

[a]Instituto de Física, Universidade Federal de Goiás, Campus Samambaia, CP 131, 74001-970, Goiânia (GO), Brazil

[b]Departamento de Física, Facultad de Bioquímica y Ciencias Biológicas, Universidad Nacional del Litoral, and Instituto de Física del Litoral (CONICET-UNL), Güemes 3450, 3000 Santa Fe, Argentina

e-mail: santana@ufg.br

MS received 14 August 2013; revised 31 October 2013; accepted 5 November 2013

**Abstract.** We report here electron paramagnetic resonance (EPR) measurements at 9 and 34 GHz, and room temperature ($T$), in powder and single crystal samples of the ternary compounds of copper nitrate or copper chloride with glycine and 1,10-phenanthroline $[Cu(Gly)(phen)(H_2O)]\cdot NO_3\cdot 1.5H_2O$ (**1**) and $[Cu(Gly)(phen)Cl]_2\cdot 7H_2O$ (**2**). In compound **1**, the copper ions are arranged in 1-D chains along one of the crystal axes connected by *syn–anti* carboxylate ligands, while in **2** the array is nearly 3-D and the connections involve $H$-bonds and stacking interactions. The angular variation of the squared $g$-factor and the line width were measured as a function of orientation of the magnetic field ($B_0$) in three orthogonal crystal planes. In both compounds we observed one resonance without hyperfine structure for any magnetic field orientation which we attribute to the collapse of the hyperfine coupling and of the resonances of two chemically identical but rotated coppers in the unit cell, produced by exchange interactions. We analyse the results in terms of the structures of the compounds and chemical paths connecting neighbour copper ions which support the exchange interactions between neighbour spins in the lattice. Considering the collapse of the EPR signals of rotated sites in the lattices we are able to set lower limits to the exchange interactions, which are supported by weak equatorial–apical carboxylate bridges in **1**, and by paths containing hydrogen bonds and aromatic $\pi$–$\pi$ interactions in **2**. Broadening due to dipole-dipole couplings and hyperfine interactions are strongly reduced by these exchange couplings and their role in the EPR line width is more difficult to recognize.

**Keywords.** Ternary copper compounds; glycine; phenanthroline; EPR; magnetic interactions.

## 1. Introduction

The synthesis and characterization of binary and ternary metal complexes are aims of supramolecular chemistry that remain active for many years. Providing information about interactions acting between molecular subunits is a subject relevant in biology and in materials science.[1] Several types of weak non-covalent interactions such as *syn–anti* carboxylate bridges,[2–5] H-bonds,[6,7] cation–$\pi$ interactions,[8,9] and $\pi$–$\pi$ stacking[10–14] are important to study biological function, and for a large variety of magnetic, electric and optical properties of materials.[15] Ternary complexes of amino acids[16] such as glycine,[17,18] L-methionine,[19] L-tyrosine, L-tryptophan, L-phenylalanine,[20] aspartic acid[21] and others, with the heteroaromatic diamine ligand 1,10-phenanthroline, show these bonds and attracted attention on preparing and characterizing metal organic frameworks. There are many investigations of their properties but questions and controversies still exist.[22] Furthermore, even though many electron paramagnetic resonance (EPR) studies in copper–amino acid and peptide compounds have been reported,[23–31] single crystal studies of the more complex ternary copper amino acid compounds are scarce,[21,32] even when this is a sensitive spectroscopic technique to investigate the electronic structure of the metal ions and to estimate the weak interactions between them supported by the non-covalent couplings mentioned before.[31]

Ternary compounds involving glycine, 1,10-phenanthroline and copper nitrate or copper chloride, named $[Cu(Gly)(phen)(H_2O)]\cdot NO_3\cdot 1.5H_2O$ (**1**) or $[Cu(Gly)(phen)Cl]_2\cdot 7H_2O$ (**2**), having $Cu^{II}$ ions connected by paths including carboxylate and stacking interactions between $Cu^{II}$ ions were reported by Zhang *et al*.[17] and Yodoshi *et al*.[18], respectively. However, no

*For correspondence

EPR studies exist for these compounds, and we report here powder and single crystal measurements analysing the results in terms of the structural characteristics and comparing them with results in similar situations.

## 2. Experimental

### 2.1 *Synthesis and crystallization of compounds **1** and **2***

All chemicals, were commercially available of analytical- or reagent-grade purity, and used as received. Compound **1** was prepared as described in ref.17 $Cu(NO_3)_2{\cdot}3H_2O$ (2 mmol, 483 mg), glycine (2 mmol, 150 mg) and NaOH (2 mmol, 80 mg) were dissolved in warm water under stirring. Ethanolic solution (5 mL) of 1,10-phenanthroline monohydrate (2 mmol, 396.4 mg) was added to the solution that was stirred for about 3 h at 60°C. The solution was maintained at room temperature and pH = 8.0, and after several weeks we obtained sky-blue rectangular prismatic crystals of **1**.

Compound **2** was prepared as described in ref.18; 140 mg (0.76 mmol) of phenanthroline were mixed with 130 mg (0.76 mmol) of $CuCl_2$ in 5 ml of 80% (v/v) methanol–water solution. The precipitate was reacted with 1.1 mg (0.015 mmol) of glycine and 1.3 mg (0.015 mmol) of $NaHCO_3$ in water solution at 70°C. The solution was maintained at room temperature and after few weeks blue prismatic crystals were obtained.

Powder X-ray measurements confirmed that the synthesized compounds **1** and **2** are those reported in references17 and18. The grown crystals of both compounds present good crystalline quality. They show well-defined *ab* crystal faces, identified by optical goniometric measurements, and have dimensions $\sim 1.80 \times 0.40 \times 0.25$ mm$^3$ for **1** and $\sim 0.80 \times 0.30 \times 0.15$ mm$^3$ for **2**.

### 2.2 *EPR measurements*

EPR measurements at room temperature in single crystal and powder samples of compounds **1** and **2** made by crushing single crystals were performed in an ESP-300 Bruker spectrometer working at 34.0 GHz (Q-band) and at 9.77 GHz (X-band), with standard Bruker cylindrical cavities operating with ∼0.4 mT of 100 kHz magnetic field modulation, and ∼19 mW of microwave power. Crystals of both samples were oriented by gluing their *ab* growth faces to a face of cleaved single crystal cubic holders of KBr with the $\boldsymbol{b}$ axis parallel to one of the sides of the cube, in order to define a laboratory orthogonal axes system $\boldsymbol{xyz}$, with $\boldsymbol{x}//\boldsymbol{a}$, $\boldsymbol{y}//\boldsymbol{b}$, $\boldsymbol{z}//\boldsymbol{c}^* = \boldsymbol{a}\times\boldsymbol{b}$. The orientation of the magnetic field $\boldsymbol{B}_0 = \mu_0\boldsymbol{H}$ in this coordinate system ($\mu_0$ is the permeability of the vacuum) was varied by rotating the sample holder with a goniometer (at 9.77 GHz), or rotating the magnet (at 34.0 GHz) with $\boldsymbol{B}_0$ in the *ab*, *bc** and *ac** planes. At each microwave frequency the EPR spectra were recorded at 5° orientation intervals for **1** and 10° for **2** of the external magnetic field in these three orthogonal planes, in a range of 180°. The magnetic field at the position of the sample was calibrated using DPPH ($g$ = 2.0036) as field marker. A single EPR line without hyperfine structure due to the copper nuclei or its ligands was observed for any orientation of $\boldsymbol{B}_0$ in the *ac**, *ab* and *bc** crystalline planes for compounds **1** and **2**. Positions and peak-to-peak line widths ($\Delta B_0$) of the resonance line were obtained by least-squares fitting the spectra to Lorentzian derivative line shapes, as expected for an exchange narrowed resonance and displayed by the observed spectra. The positions of the crystalline axes in these planes were determined within 1° from the symmetry properties of the crystal axes.

## 3. Crystal structure and exchange pathways

Compound **1** is monoclinic, space group C2/c with lattice parameters $a$ = 20.572(3) Å, $b$ = 6.9987(10) Å, $c$ = 23.561(3) Å, $\beta$ = 98.776(5)° and Z = 8 symmetry related molecules per unit cell.[17] In the basal plane the Cu ion is equatorially coordinated to nitrogen atoms N1 and N2, belonging to a 1,10-phenanthroline molecule, to nitrogen $N_3$ and oxygen $O_2$, belonging to a glycine molecule, and in an apical position to a water molecule O1w (see figure 1, obtained from the data of Zhang *et al.*[17]). The distances of the Cu ion to the $N_1$, $N_2$, $N_3$ and $O_2$ ligands are, 2.023, 1.993, 1.969, 1.950 Å, respectively while the distance to the oxygen O1w is 2.416 Å. A carboxylate oxygen $O_3$ from a neighboring glycine molecule in the sixth octahedral position which may be considered as a structural bond because of its relatively short length ($d$(Cu-$O_3$) = 2.634 Å), completes a square bipyramid. The eight symmetry related copper molecules in the unit cell of **1**, labelled as A ≡ (x,y,z), B ≡ (–x,y,1/2–z), C ≡ (1/2+x,1/2+y,z), D ≡ (1/2–x,1/2+y,1/2–z), E ≡ (–x,–y,–z), F ≡ (x,–y,–1/2+z), G ≡ (1/2–x,1/2–y,–z) and H ≡ (1/2+x,1/2–y,–1/2+z)[17], where molecules B–H are obtained from molecule A by 180° rotations around the crystallographic $\boldsymbol{b}$ axis or inversions, plus translations. In the absence of couplings between $Cu^{II}$ ions, the EPR spectra of single crystals should distinguish the resonances of $Cu^{II}$ ions related by 180° rotations, but not those related by inversions or translations. So, compound **1**

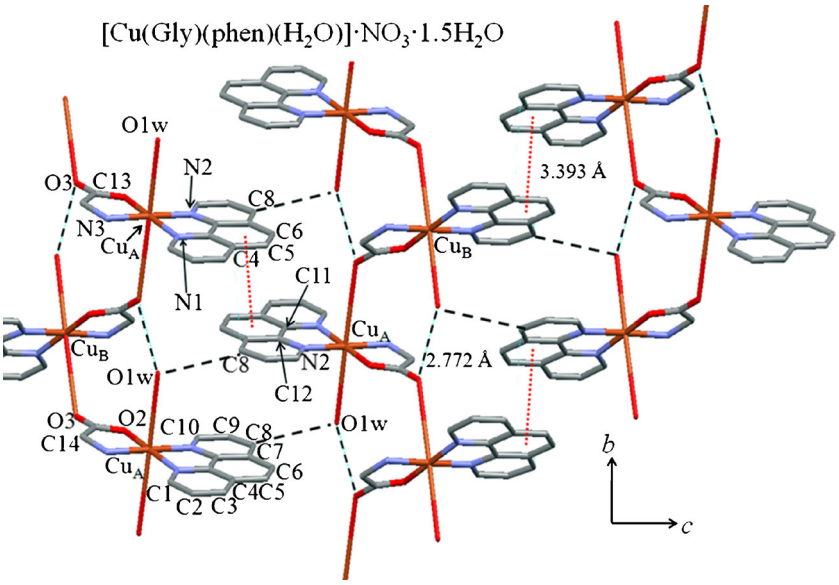


**Figure 1.** Projection on the *bc** plane of the structure of compound **1**, showing the copper molecules and the chemical paths connecting $Cu_A$ to $Cu_B$, which give rise to Cu chains along the ***b*** axis, and $Cu_A$ to $Cu_A$, connecting these chains. The dashed and dotted lines indicate the H-bonds and $\pi$–$\pi$ stacking interactions, respectively. For clarity hydrogen atoms are omitted.

should display two resonances for most orientations of $\boldsymbol{B}_0$. Exchange interactions between the $Cu^{II}$ ions may produce merging and collapse of these EPR signals, and also changes of the line width. The observed behaviour will be used below to estimate exchange interactions between $Cu^{II}$ ions.[31]

Figure 1 also shows a projection on the *bc* plane of **1** of the relevant exchange paths connecting neighbour copper ions and giving rise to $Cu^{II}$ chains along the ***b*** crystal axis. The path connecting neighbour $Cu_A$ and $Cu_B$ ions separated by 5.771 Å in **1**, contains two branches. One is an equatorial–apical *syn–anti* type carboxylate bond involving three atoms of a glycine molecule –$Cu_A$–$O2_{eq}$–C13–$O3_{ap}$–$Cu_B$–, with total length $d$ = 7.07 Å. The other branch, –$Cu_A$–O1w–H1w···O3–C13–O2–$Cu_B$–, contains a hydrogen bond and has a total length of 10.851 Å. Based on the longer path length, the presence of a H-bond, and the greater number of atoms in the path, the contribution of the second branch should be much weaker than that supported by the first branch, and its role in the exchange coupling will be neglected. Figure 1 also shows how the copper chains running parallel to the ***b*** axis are interconnected by intermolecular $\pi$–$\pi$ stacking interactions between the phenanthroline rings of adjacent molecules through the C4–C8 and C8–C4 carbons at a distance $d$ [C4–C8] = 3.393 Å.

Compound **2** belongs to the monoclinic $P2_1/n$ space group, with lattice parameters $a$ = 6.837(5), $b$ = 12.21(1), $c$ = 20.25(2) Å, $\beta$ = 95.20(3), and Z = 2,[18] and its structure is shown in figure 2. The $Cu^{II}$ ions occupy five-coordinated sites, surrounded in the equatorial plane by three nitrogen and one oxygen atoms from a bidentate phenanthroline and a glycine molecule, as in compound **1**, plus one Cl atom in the axial position. The distances of the $Cu^{II}$ ions to the N1, N2, N3, O1 and Cl atoms are 2.015, 2.014, 2.007, 1.950 and 2.573 Å, respectively. The four molecules in the unit cell of **2** at A ≡ (x,y,z), B ≡ (1/2–x,1/2+y,1/2–z), C = (−x,−y,−z) and D = (1/2+x,1/2-y,1/2+z),[18] are related by 180° rotations around the ***b***-axis, or inversion, plus translations, so there are two magnetically non-equivalent sites in the presence of an external magnetic field.

The exchange interactions between copper ions in neighbour molecules are supported by two relevant chemical paths containing one H-bond (see figure 2). The first is the equatorial–equatorial path –$Cu_A$–O1–C13–O2–H12···N3–$Cu_B$– connecting coppers at $d$ = 8.023 Å along the ***b***-direction with total length of 9.729 Å. The other is the equatorial–apical –$Cu_A$–N1–C1–C2– H2···Cl1–$Cu_B$– bond, connecting copper ions separated by 7.549 Å, with a total bond length of 11.137 Å. Other paths observed in figure 2, as –$Cu_A$–Cl1···H19–O6–H20···O1–$Cu_B$– and –$Cu_A$–N3···H11–O3–H13···Cl1–$Cu_B$–, are of equatorial-apical type connecting copper ions separated by 7.549 Å and each one includes two H-bonds. According to the rules given by Jeffrey[33] and Steiner,[34] and considering the structural

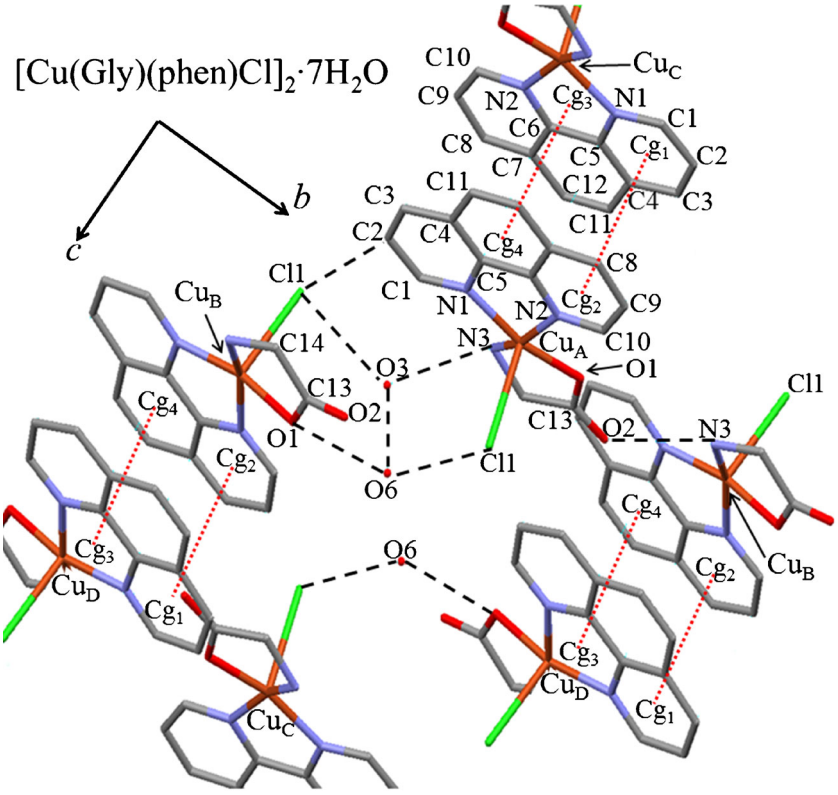


**Figure 2.** Structure and chemical paths connecting copper ions in compound **2**. Dashed and dotted lines indicate H-bonds and $\pi$–$\pi$ stacking interactions, respectively. For clarity hydrogen atoms are omitted.

data,[18] the H-bonds C2– H2· · ·Cl1 and O2· · ·H12–N3 should be weak with electrostatic interaction, and the paths Cl1· · ·H19–O6, O6–H20· · ·O1, N3· · ·H11–O3 and O3–H13· · ·Cl1 moderate and mostly electrostatic.

Neighbours $Cu_A$ and $Cu_C$, and $Cu_B$ and $Cu_D$ are connected by $\pi$–$\pi$ stacking interactions between adjacent phenanthroline rings, as well as between phenanthroline rings and five-membered chelate rings, at an average distance of 3.51 Å. These stackings, which run along the ***a***-direction and are described as Cg1(N1/C1–C5) and Cg2(N2/C6–C10) with $d$ = 3.567 Å, Cg3($Cu_A$/N1/C5/C6/N2) and Cg4(C4–C7/C11/C12) with $d$ = 3.460 Å, together with the H-bond network described above, stabilize the 3-D structure and support the magnetic interactions.[32,35] The $\pi$–$\pi$ stacking interactions (∼10 kJ mol$^{-1}$) are generally weaker than the H-bonds, (∼15–40 kJ mol$^{-1}$).[36] Paths containing two H-bonds are less effective than those with one H-bond as observed in others studies[32,35] and are not considered here. All together, they would give rise to an anisotropic 3D network of exchange couplings. As explained before, in compound **2** one should observe two EPR signals corresponding to sites A and B (or C and D), but this situation may be changed by the exchange interactions.

## 4. Results and discussion

### 4.1 *Powder EPR spectra*

The powder spectra of compounds **1** and **2** at 33.9 GHz (Q-band), are displayed in figure 3a and b, respectively. Those at 9 GHz are less resolved and not shown. The spectra are typical of $Cu^{II}$ ions with $S = \frac{1}{2}$ occupying sites with tetragonal symmetry, and do not display hyperfine structure in the $g_{//}$ region, as often occurs in compounds where the copper ions are exchange coupled, see for example figure 2 in ref. [37]. They were fitted using EasySpin,[38] a program working under Matlab[39] as described in ref. [40], using the spin Hamiltonian:

$$\mathcal{H}_S = \mu_B \boldsymbol{S}.\boldsymbol{g}.\boldsymbol{B_0}, \qquad (1)$$

where $\mu_B$ is the Bohr magneton, $\boldsymbol{S} = \frac{1}{2}$ is the effective spin operator, and $\boldsymbol{g}$ is the crystal $\boldsymbol{g}$-matrix. We consider spectra with a single resonance, consequence of the exchange interaction between $Cu^{II}$ ions in the lattice that narrows and collapses the two expected lines as explained by Anderson's theories.[41,42] The $g$-values obtained from fittings of the powder spectra at 33.9 GHz are given in table 1, and the calculated spectra are in good agreement with the experimental ones

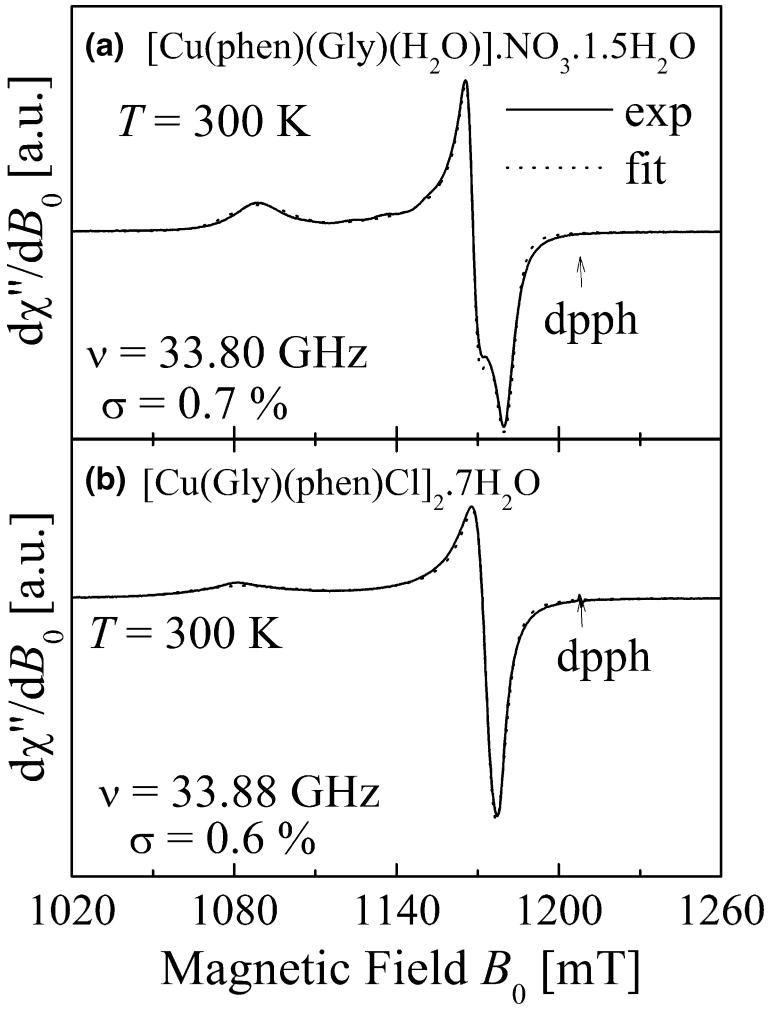


**Figure 3.** Q-band EPR spectra of powder samples of compound **1** (**a**) and **2** (**b**) measured at room temperature. Solid lines and dotted lines represent, respectively, the experimental results and the simulations obtained as explained in the text. $\sigma$ denote the quality of the spectral simulations defined by the *rms* deviations, $\sigma = [(1/N_p)\Sigma_i(S_{exp,i} - S_{sim,i})^2]^{1/2}$, where $S$ is the signal amplitudes (experimental and simulated) and the sum runs over the $N_p$ points $i$ of the spectra.

(see figure 3a and b). Small differences arise from the simplifications of the simulation which assumes that the principal directions of the ***g***-matrix and the angular variation of the line width are the same, emphasizing the convenience of EPR measurements in single crystals when the line width are anisotropic.

### 4.2 *Single crystal EPR spectra*

Figure 4a, b, c and d show spectra of single crystals of both samples obtained with $B_0$ in the $c^*b$ plane at X- and Q-bands displaying a single line in the studied planes, indicating that the exchange interactions are large enough to collapse the hyperfine splittings with the I = 3/2 spin of the copper nuclei, the I = 1 of the nitrogen ligands, and the resonance lines of the magnetically non-equivalent copper ions. Figure 5a and b display the angular variations of the squared $g$-factors of samples **1** and **2**. In the Supplementary material, figures S1 and S2 display the peak-to-peak line widths observed at 33.9 GHz. The crystal $g^2$ matrices are the averages of the molecular $g^2$ matrices of sites A and B. The experimental values of $g^2(\theta,\phi)$ at 9.8 GHz (data not shown) are similar, but less accurate than those obtained at 33.9 GHz. The spin Hamiltonian of equation 1 was least squares fitted to the data for compounds **1** and **2** in figure 5a, and b and the components of $g^2(\theta,\phi)$

**Table 1.** (a) Eigenvalues $g_1$, $g_2$, and $g_3$ of the $g$-tensor obtained from fits of the powder EPR spectra of compounds **1** and **2** at 33.9 GHz (see figure 3 and text). The components of the crystal $g^2$ matrices for compounds **1** (b) and **2** (c) are obtained by least squares fits of the function $g^2(\theta,\phi)$ to the data in single crystals, displayed in figure 5. For each compound, $(g^2)_1$, $(g^2)_2$, $(g^2)_3$ and $\boldsymbol{a_1}$, $\boldsymbol{a_2}$, $\boldsymbol{a_3}$ are the eigenvalues and eigenvectors of these $\boldsymbol{g}^2$-matrices, where $\boldsymbol{x}//\boldsymbol{a}$, $\boldsymbol{y}//\boldsymbol{b}$, $\boldsymbol{z}//\boldsymbol{c}^*$ ($\boldsymbol{c}^* = \boldsymbol{a}\times\boldsymbol{b}$). The axial directions for each compound were calculated as the normals to the planes of equatorial ligands corresponding to site A.

| (a) | $\nu$ = 33.9 GHz | | |
|---|---|---|---|
| | $g_1$ | $g_2$ | $g_3$ |
| **1** | 2.232(2) | 2.059(5) | 2.082(5) |
| **2** | 2.242(3) | 2.058(3) | 2.065(4) |
| (b) **1** | $\nu$ = 34.0 GHz | | $\nu$ = 9.77 GHz |
| $(g^2)_{xx}$ | 4.3104(9) | | 4.3227(6) |
| $(g^2)_{yy}$ | 4.9817(9) | | 4.9811(7) |
| $(g^2)_{zz}$ | 4.2612(8) | | 4.2664(5) |
| $(g^2)_{xy}$ | 0.007(1) | | 0.0196(8) |
| $(g^2)_{xz}$ | 0.039(1) | | 0.0319(8) |
| $(g^2)_{yz}$ | −0.005(1) | | −0.0152(8) |
| $(g^2)_1$ | 4.982(1) | | 4.9821(7) |
| $(g^2)_2$ | 4.240(1) | | 4.2519(7) |
| $(g^2)_3$ | 4.332(1) | | 4.3362(8) |
| $\boldsymbol{a_1}$ | [0.010(1), 1,−0.007(2)] | | [0.031(1), 1,−0.022(1)] |
| $\boldsymbol{a_2}$ | [0.481(7),−0.001(1),−0.876(4)] | | [0.409(6),−0.008(1), −0.912(3)] |
| $\boldsymbol{a_3}$ | [0.876(4),−0.005(2),0.482(7)] | | [0.912(3),−0.037(1), 0.409(6)] |
| | Axial direction | | [0.284, 0.952,−0.116] |
| $g_{//}$ | 2.252(1) | | 2.251(3) |
| $g_\perp$ | 2.059(1) | | 2.062(3) |
| $2\alpha$ | 141.2° | | 142.5° |
| $2\alpha_{cris}$ | 144.3° | | |
| (c) **2** | $\nu$ = 34.0 GHz | | $\nu$ = 9.77 GHz |
| $(g^2)_{xx}$ | 4.495(2) | | 4.424(3) |
| $(g^2)_{yy}$ | 4.241(1) | | 4.240(2) |
| $(g^2)_{zz}$ | 4.776(2) | | 4.840(3) |
| $(g^2)_{xy}$ | −0.000(2) | | −0.013(3) |
| $(g^2)_{xz}$ | −0.361(2) | | −0.336(4) |
| $(g^2)_{yz}$ | −0.003(2) | | −0.004(3) |
| $(g^2)_1$ | 5.023(2) | | 5.027(4) |
| $(g^2)_2$ | 4.241(2) | | 04.225(4) |
| $(g^2)_3$ | 4.249(2) | | 4.251(4) |
| $\boldsymbol{a_1}$ | [0.564(2),0.003(2),−0.825(1)] | | [0.487(3),0.003(3),−0.873(2)] |
| $\boldsymbol{a_2}$ | [0.4(1),0.96(5),0.2(1)] | | [0.66(5),0.65(7),0.37(3)] |
| $\boldsymbol{a_3}$ | [0.79(5),−0.2(2),0.54(3)] | | [0.57(6),−0.76(6),0.32(3)] |
| | Axial direction | | [0.894 0.138 −0.426] |
| $g_{//}$ | 2.243(3) | | 2.248(2) |
| $g_\perp$ | 2.059(3) | | 2.055(2) |
| $2\alpha$ | 168.4° | | 159.6° |
| $2\alpha_{cris}$ | 164.1° | | |

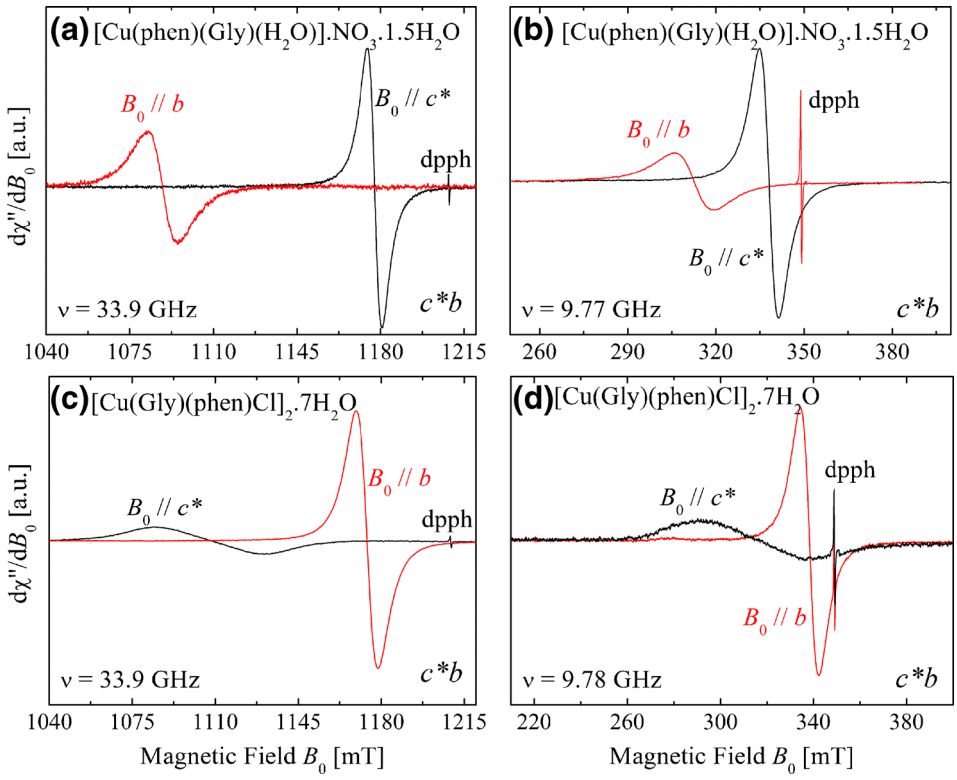


**Figure 4.** Representative experimental single crystal EPR spectra of **1** and **2**, with the magnetic field applied parallel to the *c** and *b* crystalline axis, in the *c*b* plane at room temperature. The left and right panels correspond to Q and X-bands, respectively.

obtained for **1** and **2** at each microwave frequencies using the function,

$$g^2(\theta,\phi) = (g^2)_{xx}\sin^2\theta\cos^2\phi + (g^2)_{yy}\sin^2\theta\sin^2\phi + (g^2)_{zz}\cos^2\theta + 2(g^2)_{xy}\sin^2\theta\sin\phi\cos\phi + 2(g^2)_{xz}\sin\theta\cos\theta\cos\phi + 2(g^2)_{yz}\sin\theta\cos\theta\sin\phi, \quad (2)$$

are given in table 1, which includes the eigenvalues $(g^2)_1$, $(g^2)_2$ and $(g^2)_3$, that agree with those obtained from simulations of the powder spectra and the eigenvectors of the $g^2$ matrices.The calculated values of $g^2(\theta,\phi)$ (solid lines in figure 5a, b) are in good agreement with the experiments. For **1** the *g*-factor is largest along the ***b*** axis, direction of the chains, ($g_{//} = ((g^2)_1)^{\frac{1}{2}}$ ), see figure 5a. Also, $((g^2)_2)^{\frac{1}{2}} \approx ((g^2)_3)^{\frac{1}{2}} \approx g_\perp$. Meanwhile, $g_{//}$ is in the *c*a* plane for **2**, far from the axes, so the axial symmetry of $g^2$ is less evident in figure 5b. The pattern $g_{//} > g_\perp > 2$ observed in table 1 for both compounds is consistent with the geometry of the copper ion sites suggesting a $d(x^2\text{-}y^2)$ ground orbital state,[43] as observed for other ternary compounds contaning copper and phenanthroline or other aromatic ligands.[21,44,45] Following ideas described previously,[46] the eigenvalues of the crystal $g^2$ matrices were used to obtain the molecular *g*-values for sites A and B and the angle between their apical directions, which are included in table 1. together with the crystallographic angles.

The large angular variations of the peak-to-peak line width $\Delta B_0(\theta,\phi)$ for compounds **1** and **2** observed at 9.8 and 33.9 GHz in the *ac**, *ab* and *bc** crystalline planes (figures S1 and S2) are approximately frequency independent, i.e., the observed differences between $\Delta B_0$ values at Q and X bands are less of 10% of the line width. This result indicates that the residual Zeeman interaction,[47] related to the existence of magnetically nonequivalent copper sites in the lattice[2,31,48–50] do not contribute to the EPR broadening. This result is used below to set lower limits to the magnitudes of the exchange couplings between copper ions in **1** and **2**.

### 4.3 *Discussion*

In solid paramagnetic materials the line width is frequently governed by dipolar and exchange interactions.[51,52] Dipolar interactions broaden the resonances, while exchange interactions narrow them. Another source of exchange broadening, appearing together with the collapse of the resonances of spins in symmetry related lattice sites which are magnetically non-equivalent, were discussed initially by Yokota

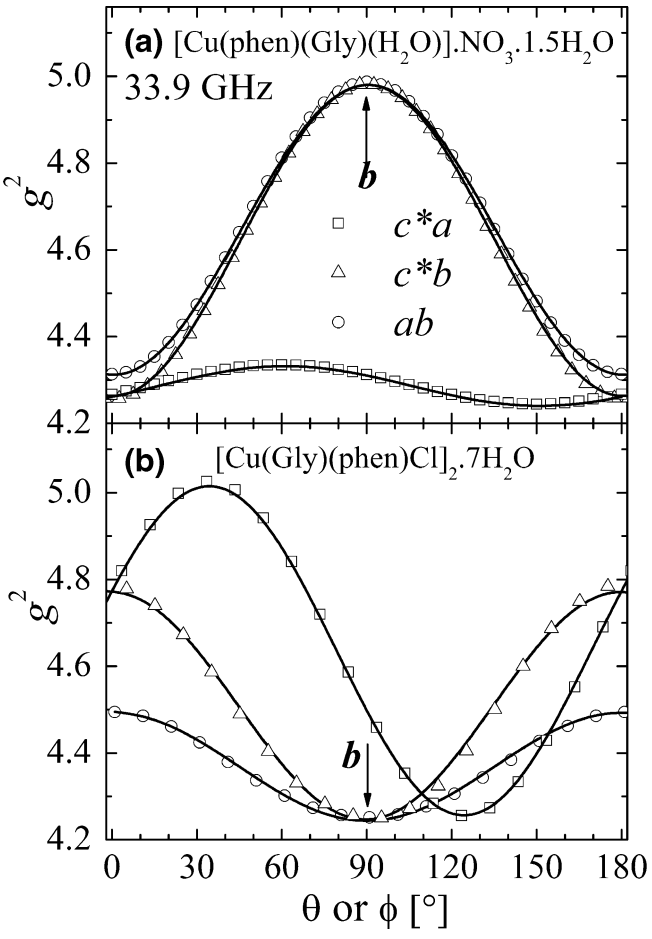


**Figure 5.** $g^2$ factors observed at 33.9 GHz and 300 K for $\boldsymbol{B}_0$ applied in the orthogonal planes $c^*a$, $c^*b$ and $ab$ in compounds **1** and **2**. The solid lines were obtained with the components of the $\boldsymbol{g}^2$ matrix given in table 1.

and Koide[53] (see also refs. 31 and 47). According Anderson's theory for the collapse of the resonances in the exchange narrowing regime, the resonances corresponding to different spins collapse when the exchange coupling equals the energy difference of the spins.[41,42] This allows setting lower limits on the magnitudes of the exchange couplings between neighbour coppers in **1** and **2** from the EPR results described above. An estimate is obtained considering the resonance condition $g\mu_B B_0 = h\nu$ and the condition given by Anderson's theory. A difference $\delta g$ in the $g$-factors of sites A and B would give rise to a distance $|\delta B| = (h\nu/\mu_B)|\delta g|/g^2$ in the fields of their resonances, and the minimum exchange interaction coupling $J$ needed to collapse these resonances is:

$$|J| \geq g\mu_B \delta B = h\nu\delta g/g,$$

where the maximun value of $\delta g$ that may occur for two symmetry related spins is $\delta g \leq g_{//} - g_{\perp}$. Thus, the condition for observing a collapsed resonance and similar linewidths at the two microwave frequencies is:

$$|J| \geq g\mu_B \delta B = h\nu\delta g/g, \text{ or,}$$
$$|J| \geq h\nu(g_{//} - g_{\perp})/g_{ave} = 3h\nu(g_{//} - g_{\perp})/(g_{//} + 2g_{\perp}).$$

Considering the $g$-values in table 1, this equation allows estimating $|J| \geq 0.12$ cm$^{-1}$ as a minimum value of the exchange couplings between neighbour coppers that could produce the full collapse of the two expected resonances observed at $\nu = 34$ GHz. This exchange coupling would collapse the spectral structure due to rotated sites in the lattice and also destroy the hyperfine structure, producing nearly frequency independent line widths. On the other hand, since the dipolar interactions are related to the distance $R$ between the interacting $Cu^{II}$ ions by $D_{dip} \approx 3\ g^2(\mu_B)^2/(2R^3)$,[11,12,51,54] one estimates $D_{dip} \sim 0.036$ cm$^{-1}$ and $\sim 0.016$ cm$^{-1}$ for compounds **1** ($d_{Cu-Cu} = 5.771$ Å ) and **2** ($d_{Cu-Cu} = 7.549$ Å ), respectively. Since this dipolar couplings are much smaller than the exchange coupling estimated above, dipolar broadening is destroyed by the exchange and considered less important. The collapse of the resonances due to rotated sites in the lattice is considered the most important consequence of the exchange coupling in **1** and **2**.

In the case of compound **1**, we may compare the lower limit $|J| \geq 0.12$ cm$^{-1}$ calculated above with the prediction $|J_{LC}| \sim 0.15$ cm$^{-1}$ of Levstein and Calvo[2] for the exchange coupling supported by a *syn–anti* carboxylate bridge with the distance of 2.634 Å for the non-covalent section of the *syn–anti* carboxylate path in **1**. The agreement supports our previous estimate. Since the spin chains in **1** are not well-isolated, as indicated by the analysis of the structure, the lineshape do not follow the predictions of Dietz *et al.*[55] for spin chains, and is mainly lorentzian.

In the case of compound **2**, as described above exchange paths with greater complexity, our magnetostructural analysis is necessarily weaker. We suggest that the magnitude of the exchange constant $J$ have the same lower limiting value as for **1**. Considering the structural data described in references 17 and 18 (see figures 1 and 2 and also figure 2 of Yoshizawa *et al.*[56]), the stacking angle is 180° for **1** and **2**, and the positive spin density of one layer is coupled to the negative spin density of the adjacent layer, and according their results the exchange interaction between the metal centres would be ferromagnetic in both compounds.

## 5. Conclusions

The *g*-matrices and the angular variation of the line width of two ternary compounds containing glycine and phenanthroline were evaluated from single crystal EPR measurements at room temperature. The result reflects magnetically coupled copper ions where the observed *g*-factor is the average of the molecular *g*-matrices of two symmetry related copper ions. The complex angular variation of the EPR line width observed in both compounds is influenced by competing broadening and narrowing mechanisms, such as magnetic dipole–dipole, hyperfine exchange and Zeeman interactions, which change the resonance line width with different angular dependences. Nevertheless, the leading role in the exchange narrowing process is the collapse of resonances due to rotated sites in the lattice. Considering this collapse, we estimate in the case of compound **1** a lower limit for the exchange coupling between copper neighbours that supports predictions of an earlier study of *syn–anti* carboxylate bridges. Our investigation also provides update on the role of the hydrophobic interactions to support exchange interactions, but more theoretical work and experimental studies in compounds with copper ions connected by $\pi$–$\pi$ stacking or H-bondings should be performed.

## Supplementary information

Electronic supplementary information (figures S1 and S2) can be found in www.ias.ac.in/chemsci.

## Acknowledgements

This work was supported by CNPq in Brazil and by CAI+D-UNL in Argentina. RC is a researcher of CONICET.

## References

1. Grisser T and Sigel H 1970 *Inorg. Chem.* **9** 1238 and references therein
2. Levstein P R and Calvo R 1990 *Inorg. Chem.* **29** 1581
3. Colacio E, Dominguez-Vera J M, Costes J P, Kivekäs R, Laurent J P, Ruiz J and Sundberg M 1992 *Inorg. Chem.* **31** 774
4. Colacio E, Dominguez-Vera J M, Kivekäs R, Moreno J, Romerosa M A and Ruiz J 1993 *Inorg. Chim. Acta* **212** 115
5. Colacio E, Domínguez-Vera J M, Mustapha Ghazi M, Kivekäs R, Klinga M and Moreno J M 1999 *Eur. J. Inorg. Chem.* 441
6. Jeffrey, G A 1997 *An introduction to hydrogen bonding* (New York: Oxford University Press)
7. Steiner T 2002. *Angew. Chem. Int. Ed.* **41**(48)
8. (a) Dougherty, D A 1996 *Science* **271** 163–168; (b) Ma, J C and Dougherty, D A 1997 *Chem. Rev.* **97** 1303
9. Mahadevi A S and Sastry G N 2013 *Chem. Rev.* **113** 2100
10. Hunter C A 1994 *Chem. Soc. Rev.* 101
11. Subramanian P S, Suresh E, Dastidar P, Waghmode S and Srinivas D 2001 *Inorg. Chem.* **40** 4291
12. Subramanian P S, Suresh E and Srinivas D 2000 *Inorg. Chem.* **39** 2053
13. Terrón A, Fiol J J, García-Raso A, Barceló-Oliver M and Moreno V 2007 *Coord. Chem. Rev.* 1973
14. Hong L, Yu L, Zhang S -G, Wang Y-Q and Shi J-M 2012 *Chin. J. Struc. Chem.* 285
15. Lehn J-M 1995 *Supramolecular chemistry, Concepts and perspectives* Weinheim, VCH
16. Shimazaki Y, Takani M and Yamauchi O 2009 *Dalton Trans.* 7854
17. Zhang S and Zhou J 2008 *J. Coord. Chem.* **61** 2488
18. Yodoshi M, Odoko M and Okabe N 2007 *Chem. Pharm. Bull.* **55** 853
19. Martin-Polo J J, Driessen W L, Cervantes-Lee F and Mendoza-Díaz G 1995 *J. Inorg. Biochem.* **59** 53
20. Sugimori T, Masuda H, Ohat N, Koiwai K, Odani A and Yamauchi O 1997 *Inorg. Chem.* **36** 576
21. Brondino C D, Calvo R, Atria A M, Spodine E, Nascimento O R and Peña O 1997 *Inorg. Chem.* **36** 3183
22. Grimme S 2008 *Angew. Chem. Int. Ed.* **47** 3430
23. Calvo R, Mesa M A, Oliva G, Zukerman-Schpector J, Nascimento O R, Tovar M and Arce R 1984 *J. Chem. Phys.* **81** 4584
24. Gennaro A M, Levstein P R, Steren C A and Calvo R 1987 *Chem. Phys.* **111** 431
25. Levstein P R, Calvo R, Castellano E E, Piro O E and Rivero B E 1990 *Inorg. Chem.* **29** 3918
26. Calvo R, Levstein P R, Castellano E E, Fabiane S B, Piro O E and Oseroff S B 1991 *Inorg. Chem.* **30** 216
27. Calvo R, Passeggi M C G, Novak M A, Symko O G, Oseroff S B, Nascimento O R and Terrile M C 1991 *Phys. Rev. B* **43** 1074
28. Costa-Filho A J, Nascimento O R, Ghivelder L and Calvo R 2001 *J. Phys. Chem. B* **105** 5039
29. Santana R C, Cunha R O, Carvalho J F, Vencato I and Calvo R 2005 *J. Inorg. Biochem.* **99** 415
30. Chagas E F, Rapp R E, Rodrigues D E, Casado N M C and Calvo R 2006 *J. Phys. Chem. B* **110** 8052
31. Calvo R 2007 *Appl. Magn. Reson.* **31** 271
32. Brondino C D, Calvo R, Atria A M, Spodine E V and Peña O 1995 *Inorg. Chim. Acta* **228** 261
33. Jeffrey G A 1997 *An introduction to hydrogen bonding* (New York: Oxford University Press)
34. Steiner T 2002 *Angew. Chem. Int. Ed.* **41** 48
35. Costa-Filho A J, Munte C E, Barberato C, Castellano E E, Mattioli M P D, Calvo R and Nascimento O R 1999 *Inorg. Chem.* **38** 4413
36. Jorgensen W L and Severance D L 1990 *J. Am. Chem. Soc.* **112** 4768

37. Balagopalakrishna C and Rajasekharan M V 1990 *Phys. Rev. B* **42** 7794
38. Stoll S and Schweiger A 2006 *J. Magn. Reson.* **178** 42
39. Matlab *The Mathworks Inc, MA: Natick 01760*
40. Gerard M F, Aiassa C, Casado N M C, Santana R C, Perec M, Rapp R E and Calvo R 2007 *J. Phys. Chem. Sol.* **68** 1533
41. Anderson P W and Weiss P R 1953 *Rev. Mod. Phys.* **25** 269
42. Anderson P W 1954 *J. Phys. Soc. Jpn.* **9** 316
43. Hathaway B J, Wilkinson G, Gillard R D and McCleverty J A (eds) 1987 *Comprehensive coordination chemistry*, vol. 5, Oxford, UK: Pergamon Press
44. Battaglia L P, Corradi A B, Zoroddu M A, Manca G, Basosi R and Solinas C 1991 *J. Chem. Soc. Dalton Trans.* 2109
45. Neuman N I, Franco V G, Ferroni F M, Baggio R, Passeggi M C G, Rizzi A C and Brondino C D 2012 *J. Phys. Chem. A* **116** 12314
46. Calvo R and Mesa M A 1982 *Phys. Rev. B* **28** 1244
47. Passeggi M C G and Calvo R 1995 *J. Magn. Reson. A* **114** 1
48. Levstein P R, Steren C A, Gennaro A M and Calvo R 1988 *Chem. Phys.* **120** 449
49. Steren C A, Gennaro A M, Levstein P R and Calvo R 1989 *J. Phys. Condens. Matter* **1** 637
50. Gennaro A M and Calvo R 1989 *J. Phys.: Condens. Matter* **1** 7061
51. Abragam A, Bleaney B 1970 *Electron paramagnetic resonance of transition ions* (Cambridge: Oxford University Press)
52. Bencini A, Gatteschi D 1990 *Electron paramagnetic resonance of exchange coupled systems* (Berlin: Springer-Verlag)
53. Yokota M and Koide S 1953 *J. Phys. Soc. Jpn.* **9** 953
54. Fedin M V, Zhilina E F, Chizhov D L, Apolonskaya I A, Aleksandrov G G, Kiskin M A, Sidorov A A, Bogomyakov A S, Romanenko G V, Eremenko I L, Novotortsev V M and Charushin V N 2013 *Dalton. Trans.* **42** 4513
55. Dietz R E, Merrit F R, Dingle R, Hone D, Silbernagel B G and Richards P M 1971 *Phys. Rev. Lett.* **26** 1186
56. Yoshizawa K and Hoffmann R 1995 *J. Am. Chem. Soc.* **117** 6921